

## Disorder-Induced Static Antiferromagnetism in Cuprate Superconductors

Brian M. Andersen,<sup>1</sup> P. J. Hirschfeld,<sup>1</sup> Arno P. Kampf,<sup>2</sup> and Markus Schmid<sup>2</sup>

<sup>1</sup>*Department of Physics, University of Florida, Gainesville, Florida 32611-8440, USA*

<sup>2</sup>*Theoretische Physik III, Elektronische Korrelationen und Magnetismus, Institut für Physik, Universität Augsburg, 86135 Augsburg, Germany*

(Received 20 December 2006; published 2 October 2007)

Using model calculations of a disordered  $d$ -wave superconductor with on-site Hubbard repulsion, we show how dopant disorder can stabilize novel states with antiferromagnetic order. We find that the critical strength of correlations or impurity potential necessary to create an ordered magnetic state in the presence of finite disorder is reduced compared to that required to create a single isolated magnetic droplet. This may explain why, in cuprates such as  $\text{La}_{2-x}\text{Sr}_x\text{CuO}_4$ , low-energy probes have identified a static magnetic component which persists well into the superconducting state, whereas, in cleaner systems such as  $\text{YBa}_2\text{Cu}_3\text{O}_{6+\delta}$ , it is absent or minimal.

DOI: [10.1103/PhysRevLett.99.147002](https://doi.org/10.1103/PhysRevLett.99.147002)

PACS numbers: 74.72.-h, 74.25.Ha, 74.25.Jb, 74.81.-g

The occurrence of high-temperature superconductivity in cuprates near the antiferromagnetic (AF) phase of the parent compounds has prompted speculation since their discovery that superconductivity and magnetism were intimately related. For the most part, it has been assumed that the two forms of order compete and do not coexist, consistent with the vanishing of the Néel temperature  $T_N$  before the onset of a superconducting critical temperature  $T_c$  and the suppression of  $T_c$  near doping  $x = 1/8$ , where static stripe phases can be stable [1]. On the other hand, there have been persistent reports of static AF at low temperatures  $T$  in the superconducting phase at low doping, as measured by muon spin resonance ( $\mu\text{SR}$ ) [2,3], nuclear magnetic resonance (NMR) [4,5], and elastic neutron scattering (NS) [6,7]. The NS experiments reveal an incommensurate (IC) ordering wave vector evident by a quartet of peaks surrounding  $(\pi, \pi)$ . Since the neutron response is enhanced by an applied magnetic field [6,8,9], several authors have discussed it in terms of coexisting  $d$ -wave superconductivity (dSC) and field-induced spin density waves [10]. Recent magnetic Raman scattering data on  $\text{La}_{2-x}\text{Sr}_x\text{CuO}_4$  (LSCO) have been discussed in terms of such effects as well [11]. However, static order also exists at zero field in the underdoped phase of LSCO [6,7] and has been attributed to disorder [6]. In optimally doped LSCO, Kimura *et al.* [12] did not detect ordered moments in pure and 1% Zn-substituted samples. An elastic peak similar to the pure underdoped material was observed when 1.7% Zn was added, however [12].

Phenomena similar to those in LSCO have been observed in other materials, e.g.,  $\text{Y}_{1-x}\text{Ca}_x\text{Ba}_2\text{Cu}_3\text{O}_6$  and  $\text{Bi}_2\text{Sr}_2\text{CaCu}_2\text{O}_{8+x}$  (BSCCO), where  $\mu\text{SR}$  directly reveals a slowing down and subsequent freezing of spin fluctuations as  $T$  is lowered [2,13]. On the other hand, experiments on optimally doped  $\text{YBa}_2\text{Cu}_3\text{O}_{6+\delta}$  (YBCO), even with significant percentages of Zn, have never detected static magnetic signals. While there have been reports of AF coexisting with dSC in underdoped YBCO, recent NS measurements on  $\text{YBCO}_{6.5}$  found that AF order, while

static from the point of view of NS time scales  $10^{-10}$  s, was fluctuating faster than the time scale  $10^{-6}$  s for  $\mu\text{SR}$ . Thus, it appears that, while in YBCO low-frequency AF fluctuations are present, they do not “freeze out.” Recently, reports of static magnetism in this system near O content 6.35, close to the onset of superconductivity, have been reported by  $\mu\text{SR}$  [14,15] but are still controversial; the main point is that the spin-glass phase is minimal in YBCO compared to LSCO [16]. There are many differences between YBCO and the other cuprates, of course, but most importantly YBCO appears to be the cleanest material because the O dopants can order in the CuO chains. LSCO, on the other hand, is doped by randomly located charged Sr ions only 2.4 Å away from the CuO<sub>2</sub> planes. Therefore, it seems likely that disorder itself may be responsible for inducing the magnetism in zero field in LSCO and possibly part of the magnetic field dependence as well.

$\mu\text{SR}$  experiments [3] indicate that several changes occur with decreasing  $T$  for a given sample: one where random freezing of moments occur and a second where a sharply peaked magnetization distribution arises. We propose that the first is due to the creation of isolated AF droplets and the second to the formation of networks of such states which exhibit quasi-long-range order. The latter is a subtle process, which, even for a single pair of impurities, depends on the relative orientation and distance of impurity positions [17]. However, the basic physics of ordering is easy to understand. In one dimension, Shender and Kivelson [18] pointed out that the interactions between impurities in a quantum spin chain are nonfrustrating: If an impurity creates a local AF droplet, a second one can always orient itself to avoid losing exchange energy. In two dimensions (2D), this continues to apply for spin models with nearest neighbor exchange but may break down in the presence of mobile charges.

Below, we study the disorder-induced magnetization in a dSC with correlations described by the Hubbard model treated in an unrestricted Hartree-Fock approximation.

We focus on important qualitative differences between the clean and the dirty limits of both the underdoped and the optimally doped regimes. Specifically, we show that, with a fixed choice of realistic parameters, as in LSCO, the magnetism is present at low doping, disappears at optimal doping, but can be recreated with a small concentration of strong scatterers. For YBCO, such effects are absent since the disorder potential in the CuO<sub>2</sub> planes is negligible and independent of doping. This result agrees with a recently proposed origin of the unusual transport measurements in LSCO compared to YBCO [19,20].

*Model.*—The Hamiltonian, defined on a 2D lattice, is

$$\hat{H} = - \sum_{\langle ij \rangle \sigma} t_{ij} \hat{c}_{i\sigma}^\dagger \hat{c}_{j\sigma} + \sum_{i\sigma} (U n_{i,-\sigma} + V_i^{\text{imp}} - \mu) \hat{c}_{i\sigma}^\dagger \hat{c}_{i\sigma} + \sum_{\langle ij \rangle} (\Delta_{ij} \hat{c}_i^\dagger \hat{c}_j^\dagger + \text{H.c.}). \quad (1)$$

Here  $\hat{c}_{i\sigma}^\dagger$  creates an electron on site  $i$  with spin  $\sigma$ ,  $t_{ij} = \{t, t', t''\}$  denote the three nearest neighbor hopping integrals,  $V_i^{\text{imp}} = \sum_{j=1}^N V^{\text{imp}} \delta_{ij}$  is a nonmagnetic impurity potential resulting from a set of  $N$  pointlike scatterers of strength  $V^{\text{imp}}$ ,  $\mu$  is the chemical potential adjusted to fix the doping  $x$ , and  $\Delta_{ij}$  is the  $d$ -wave pairing potential between sites  $i$  and  $j$ . The amplitude of  $\Delta_{ij}$  is set by the dSC coupling constant  $V_d$  [21]. We fix the band  $t' = -0.4t$  and  $t'' = 0.12t$ , giving the Fermi surface shown in Fig. 1(a). We have solved Eq. (1) self-consistently by diagonalizing the associated Bogoliubov-de Gennes equations in the  $T = 0$  limit on  $34 \times 34$  systems [21].

Equation (1) has been used extensively to study bulk competing phases, field-induced magnetization, as well as novel bound states at interfaces between AF and superconductors [22]. It has also been used to study field-induced moment formation around nonmagnetic impurities in the correlated dSC [17,23], with considerable success at fitting NMR line shapes [21] in Li- and Zn-substituted YBCO. Interference effects of these paramagnetic states, while significant, are less important than in the heavily disordered case studied in this Letter where the ground state in zero field exhibits local magnetism.

*Results.*—For clean systems, it is well known that there exists a large region in  $(U, V_d, T)$  space dominated by spin and charge ordered stripe states of coexisting dSC and AF order [22]. For fixed  $V_d$  and  $T$ , we denote by  $U_{c2}$  the critical Coulomb repulsion for entering this bulk magnetic

state; i.e., for  $U < U_{c2}$ , in the absence of disorder, the ground state is a homogeneous dSC.

For a single nonmagnetic impurity [24], there exists a lower critical  $U_{c1}$  such that local impurity-induced magnetization exists for  $U_{c1} < U < U_{c2}$  [25] as shown in Fig. 1(b). In general,  $U_{c1}$  depends on the impurity strength  $V^{\text{imp}}$  [17,21]. However, already for two impurities interference effects modify the 1-impurity phase diagram [17]. The magnetic structure factor  $S(q)$  associated with the AF droplet in Fig. 1(b) is shown in Fig. 1(c). It is dominated by four IC peaks along the diagonals, a result which is, however, sensitive to the input parameters.

We now turn to the many-impurity situation. In the following model for LSCO, the Sr ions are assumed to be the primary source of disorder, such that  $n^{\text{imp}} = x$ , where  $n^{\text{imp}}$  denotes the impurity concentration. These systems are in the strongly disordered regime, where the Fermi wavelength  $\lambda_F$  is comparable to the average distance between the dopants, such that the disorder is far from the 1-impurity limit and novel emergent spin-glass states can arise. Since the Sr dopants are removed from (but close to) the CuO<sub>2</sub> planes, we model them as intermediate strength scatterers with  $V^{\text{imp}} = 3.0t$  (below, we use  $V^{\text{dop}}$  to indicate the Sr potential). Figure 2(a) shows the simplest schematic picture of disorder stabilization of a single Néel phase [18] by nonmagnetic impurities. Not all impurities in the correlated system need “magnetize” for a given  $U$ , however: In the disordered system, the effective criterion to drive the impurity through the local magnetic phase transition is different for each impurity. Increasing the repulsion  $U$  then increases the concentration of impurities which induce a local magnetization droplet, as shown in Figs. 2(b) and 2(c). With further increase of  $U$ , the system evolves from a state with dilute nonoverlapping AF droplets to connected spin textures [Fig. 2(d)]. The resulting patterns exhibit AF domain structure and are more complex than suggested in Fig. 2(a), due to frustration induced by the charge degrees of freedom in Eq. (1) and/or glassy supercooling effects.

While the current mean field treatment of the Hubbard model does not faithfully capture the band narrowing due to correlations near half-filling which leads to the Mott transition, it may be expected that underdoped systems are characterized by larger effective interactions. In our picture for LSCO, the  $x$  dependence of the spin order is therefore described qualitatively by the sequence  $2(d) \rightarrow 2(c) \rightarrow 2(b)$ , until it disappears completely at effective  $U$ 's below

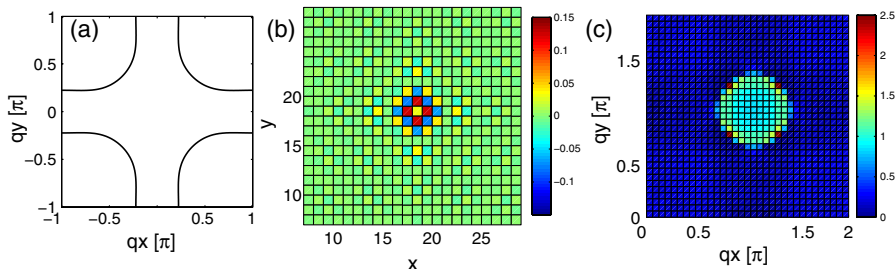


FIG. 1 (color online). (a) Fermi surface with  $x = 7.5\%$  for the band used in this Letter. For this band, the critical value for bulk order is  $U_{c2} = 3.50t$ . (b),(c) Magnetization and structure factor  $S(q)$  for a single pointlike scatterer  $V^{\text{imp}} = 3.0t$  for  $x = 7.5\%$  and  $U = 3.3t$ . For these parameters,  $U_{c1} = 3.25t$ .

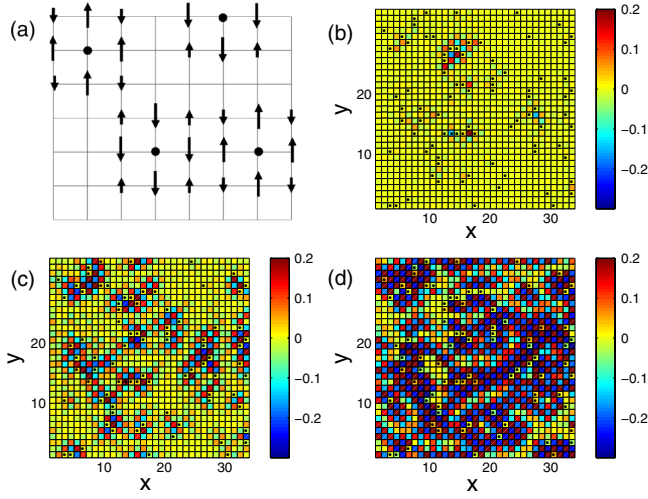


FIG. 2 (color online). (a) Schematic: Stabilization of a single Néel phase by impurities. (b)–(d) Disorder-induced magnetization for a single fixed impurity configuration with  $x = 7.5\%$  and (b)  $U = 2.8t$ , (c)  $U = 3.2t$ , and (d)  $U = 3.6t$ . In (a)–(d), the black dots indicate the impurity or dopant positions.

$U_{c1}$  near optimal doping. Increasing  $x$  should also be accompanied by a weakening of the Sr potential  $V^{\text{dop}}$  due to enhanced screening. Within our model, increasing  $U$  or  $V^{\text{dop}}$  leads to qualitatively similar results, and we cannot determine from this approach which effect is dominant in real systems. Note from Fig. 2 that AF droplets are induced for  $U \gtrsim 2.4t$ , a substantially reduced critical value compared to the 1-impurity case in Fig. 1. This is because the Hubbard correlations induce charge redistributions which alter the effective local chemical potential, such that the criterion for the magnetization of each impurity depends on its local disorder environment. Some regions containing impurities have charge densities closer to the phase boundary for AF order, thus enhancing local moment formation relative to the single impurity case. In the limit of large  $U$ , the magnetic order becomes qualitatively similar to that arising in a stripe state with quenched disorder [26].

In Figs. 3(a) and 3(b), we show the inhomogeneous electronic density and dSC gap corresponding to Fig. 2(c). The repulsive Sr dopants locally suppress both quantities, which are therefore anticorrelated with the induced spin order. As expected, the gap varies more smoothly compared to the density due to the coherence length  $\xi$  of the dSC condensate. The magnetic structure factor  $S(q)$  (averaged over 30 distinct impurity configurations) associated with the disorder-induced magnetic order in Figs. 2(b) and 2(d) is shown in Figs. 3(c) and 3(d), respectively. It is dominated by an IC ring surrounding  $(\pi, \pi)$  with an intensity distribution similar to the single impurity  $S(q)$  for the dilute case [Fig. 3(c)], but which rotates into a + shaped pattern for the connected spin textures at larger  $U$  [Fig. 3(d)]. This implies a rotation (and weakening) of the IC pattern close to the region where the static order

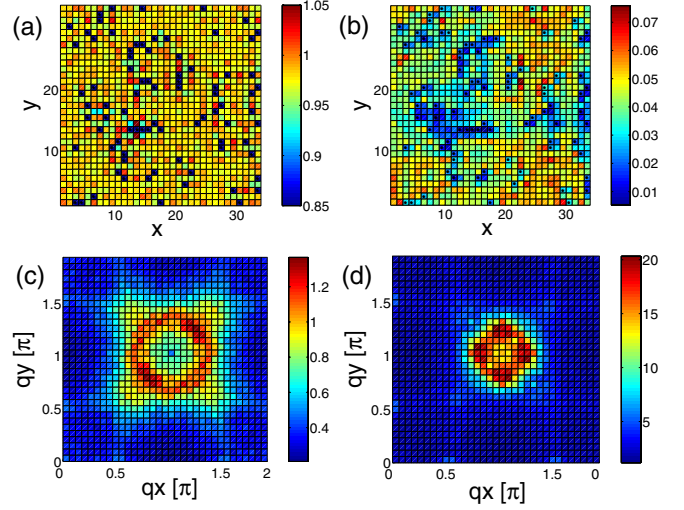


FIG. 3 (color online). (a) Electronic density and (b) dSC gap for the parameters shown in Fig. 2(c). (c),(d) display the impurity-averaged magnetic structure factor  $S(q)$  for the dilute magnetic droplet limit (small  $U$ ) and dense limit (large  $U$ ) corresponding to Figs. 2(b) and 2(d), respectively.

disappears. As mentioned above, such details are, however, sensitive to, e.g., the specific band parameters [27].

Last, we discuss optimally doped LSCO where static AF is absent in nominally clean samples, but where it can be induced by magnetic fields [6] or critical concentrations of strong scatterers. For instance, Kimura *et al.* [12] found that for  $x = 0.15$  it takes approximately 2% Zn to induce IC peaks in the NS diffraction. Below this critical concentration, there was no measurable signal above the background. We have simulated this situation by solving Eq. (1) with  $x = 0.15$  in the presence of 1% and 2% randomly

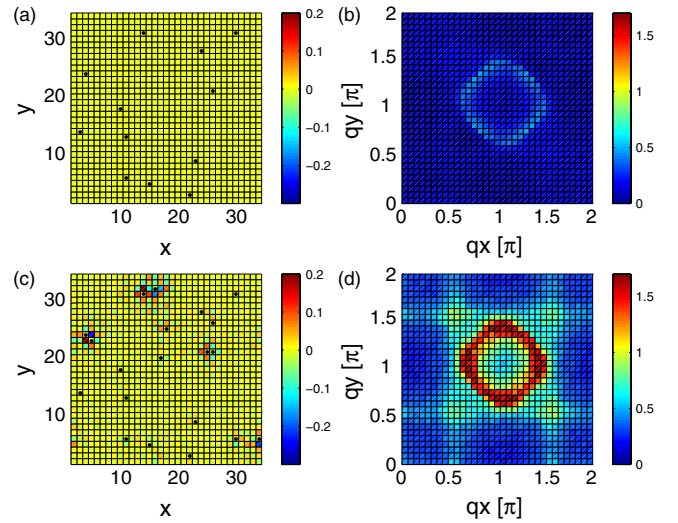


FIG. 4 (color online). Induced magnetization (left) and impurity-averaged  $S(q)$  (right) for  $U = 3.2t$  with a 1% (top) and 2% (bottom) concentration of randomly distributed strong scatterers. Note that the figures are shown on the same scale. For clarity, the black dots (left) show only the Zn positions.

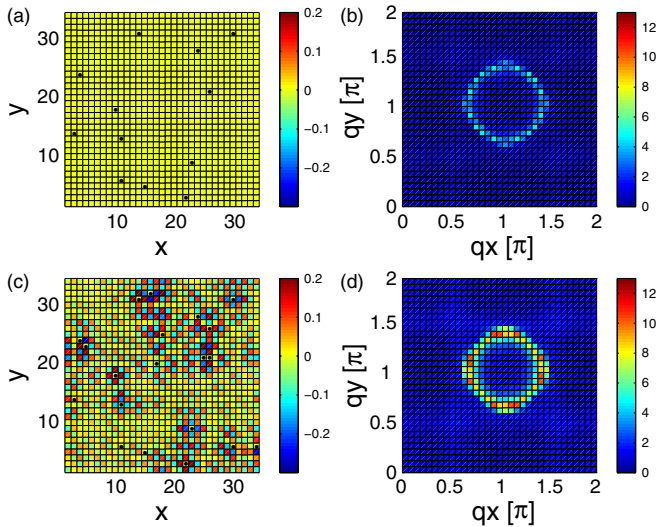


FIG. 5 (color online). Same as Fig. 4 but for  $U = 3.4t$ .

distributed strong scatterers ( $V^{\text{Zn}} = 100t$ ) in addition to the  $n^{\text{imp}} = 15\%$  weak ( $V^{\text{dop}} = 1t$ ) dopant impurities. As mentioned above, the weaker  $V^{\text{dop}}$  compared to the underdoped case is expected from an enhanced screening of the Sr potential at optimal doping. For a single Zn impurity, magnetization is induced only for  $U \geq 3.35t$ . The many-impurity results including both  $V^{\text{dop}}$  and  $V^{\text{Zn}}$  are shown for different Coulomb repulsions in Figs. 4 and 5. For systems with 1% Zn, Figs. 4(a) and 4(b) reveal a negligible induced magnetization. However, as seen from Figs. 4(c) and 4(d), simply adding enough strong scatterers can induce sizable local magnetic order. It is remarkable that such a small difference in the concentration can induce magnetism similar to the experimental observations. The number of Zn ions that induce AF droplets depends on the Hubbard  $U$  as seen by comparing Figs. 4 and 5. The resulting disorder-averaged  $S(q)$  agrees well with the NS measurements in Ref. [12].

**Conclusions.**—The interplay of dopant disorder and electronic correlations can induce novel magnetic states, which we propose exist in intrinsically disordered cuprates such as LSCO and BSCCO, in contrast to the cleaner YBCO system. Last, we showed that small concentrations of Zn can induce a similar magnetic state which has apparently been observed in NS experiments on optimally doped LSCO. An obvious question is to what extent the magnetic state influences the scattering of quasiparticles in the dSC and normal states. Studies along these lines are in progress.

We acknowledge useful discussions with I. Affleck, M. Gabay, P. Hedegård, B. Keimer, T. Kopp, C. Panagopoulos, and N. Trivedi. P.J.H. and B.M.A. were supported in part by DOE Grant No. DE-FG02-05ER46236. A.P.K. and M.S. acknowledge support

through SFB 484 of the DFG.

- [1] J. Tranquada *et al.*, Nature (London) **375**, 561 (1995).
- [2] C. Panagopoulos *et al.*, Phys. Rev. B **66**, 064501 (2002).
- [3] C. Panagopoulos and V. Dobrosavljević, Phys. Rev. B **72**, 014536 (2005).
- [4] V.F. Mitrović *et al.*, Phys. Rev. B **67**, 220503(R) (2003).
- [5] K. Kakuyanagi *et al.*, Phys. Rev. Lett. **90**, 197003 (2003).
- [6] B. Lake *et al.*, Nature (London) **415**, 299 (2002).
- [7] S. Wakimoto *et al.*, Phys. Rev. B **63**, 172501 (2001).
- [8] B. Lake *et al.*, Science **291**, 1759 (2001).
- [9] B. Khaykovich *et al.*, Phys. Rev. B **66**, 014528 (2002).
- [10] E. Demler, S. Sachdev, and Y. Zhang, Phys. Rev. Lett. **87**, 067202 (2001); M. Franz, D.E. Sheehy, and Z. Tešanović, *ibid.* **88**, 257005 (2002); J.X. Zhu, I. Martin, and A.R. Bishop, *ibid.* **89**, 067003 (2002); A. Ghosal, C. Kallin, and A.J. Berlinsky, Phys. Rev. B **66**, 214502 (2002); B.M. Andersen, P. Hedegård, and H. Bruus, *ibid.* **67**, 134528 (2003).
- [11] L.H. Machtoub, B. Keimer, and K. Yamada, Phys. Rev. Lett. **94**, 107009 (2005).
- [12] H. Kimura *et al.*, Phys. Rev. Lett. **91**, 067002 (2003).
- [13] Ch. Niedermayer *et al.*, Phys. Rev. Lett. **80**, 3843 (1998).
- [14] S. Sanna *et al.*, Phys. Rev. Lett. **93**, 207001 (2004).
- [15] R.I. Miller *et al.*, Physica (Amsterdam) **374B–375B**, 215 (2006).
- [16] J. Bobroff *et al.*, Phys. Rev. Lett. **89**, 157002 (2002).
- [17] Y. Chen and C.S. Ting, Phys. Rev. Lett. **92**, 077203 (2004).
- [18] E.F. Shender and S.A. Kivelson, Phys. Rev. Lett. **66**, 2384 (1991).
- [19] B.M. Andersen and P.J. Hirschfeld, Physica (Amsterdam) **460C**, 744 (2007).
- [20] X. Sun *et al.*, Phys. Rev. Lett. **96**, 017008 (2006).
- [21] J.W. Harter *et al.*, Phys. Rev. B **75**, 054520 (2007).
- [22] I. Martin *et al.*, Int. J. Mod. Phys. B **14**, 3567 (2000); M. Ichioka, M. Takigawa, and K. Machida, J. Phys. Soc. Jpn. **70**, 33 (2001); Y. Chen *et al.*, Phys. Rev. Lett. **89**, 217001 (2002); B.M. Andersen and P. Hedegård, *ibid.* **95**, 037002 (2005); H.-Y. Chen and C.S. Ting, Phys. Rev. B **71**, 220510(R) (2005); B.M. Andersen *et al.*, *ibid.* **72**, 184510 (2005); M. Mayr, arXiv:cond-mat/0604636.
- [23] Y. Ohashi, Phys. Rev. B **66**, 054522 (2002).
- [24] A.V. Balatsky, I. Vekhter, and J.-X. Zhu, Rev. Mod. Phys. **78**, 373 (2006).
- [25] H. Tsuchiura *et al.*, Phys. Rev. B **64**, 140501 (2001); Z. Wang and P.A. Lee, Phys. Rev. Lett. **89**, 217002 (2002).
- [26] J.A. Robertson *et al.*, Phys. Rev. B **74**, 134507 (2006); A. Del Maestro, B. Rosenow, and S. Sachdev, *ibid.* **74**, 024520 (2006); W.A. Atkinson, *ibid.* **71**, 024516 (2005); M. Vojta, T. Vojta, and R.K. Kaul, Phys. Rev. Lett. **97**, 097001 (2006).
- [27] For example, the band  $t' = -0.3$ ,  $t'' = 0.0$  exhibits + shaped IC patterns in both the small and the large  $U$  limit.